Automatic Segmentation of the Epicardium in Late Gadolinium Enhanced Cardiac MR Images

Kjersti Engan[1], Valery Naranjo[2], Trygve Eftesøl[1], Stein Ørn[3], Leik Woie[3]

[1] University of Stavanger, Stavanger, Norway
[2] Labhuman, I3BH, Universitat Politècnica de València, Valencia, Spain
[3] Stavanger University Hospital, Stavanger, Norway

Abstract

A novel method for fully automatic segmentation of the epicardium of the left ventricle in Late Gadolinium Enhanced Cardiac MR images (LGE-CMR), short axis view is presented. No other images or measurements are used. The method uses prior information about typical heart size and shape making an a priori probability map around the automatically detected heart center (HC). An a posteriori probability map is made iteratively by combining the current probability model with the preprocessed image and low-pass filtering over consecutive slices. The a posteriori probability map is used as the input for segmentation. Using the detected HC as origin, a radial evaluation is performed for all possible angles $[0 - 2\pi]$*, giving a candidate border point on the epicardium. The final segmentation combines the information from all slices. The presented method is tested on all slices of 54 patients, and gives a mean Dice index of 0.86 and mean Jaccard index of 0.76.*

1. Introduction

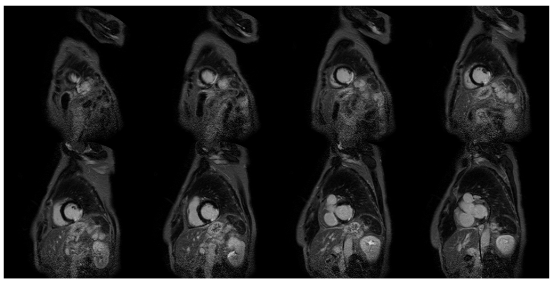

Figure 1. Consecutive MRI slices of an example patient with myocardial scar.

Late Gadolinium Enhanced Cardiac Magnetic Resonance images (LGE-CMR) are used to assess the scarred areas of the myocardium after a myocardial infarction. Healthy myocardium appears very dark in CMR images, however the edges of the heart in LGE-CMR images where the patient has a scar in the myocardium are sometimes very weak or non-existing since the scarred areas will take intensity levels close to the blood pool or the surrounding areas. This makes automatic segmentation of the myocardium in LGE-CMR images difficult. In many hospitals today the segmentation of the myocardial muscle is performed manually or semi-automatically by expert cardiologists. This can be time-consuming work, and the results will have a degree of inter- and intra-observer variability. There have been attempts to solve the problem of automatic segmentation reported in the literature, but to the authors knowledge a fully automatic method for segmenting LGE-CMR images does not exist today. Some methods require manual input in form of landmarks or cropping of region of interest etc. seems to be necessary [1, 2]. Others make use of additional data as the corresponding cine CMR [3, 4].

This work proposes a new method for automatic segmentation of the epicardium. A priori knowledge of typical heart size and shape is used as the input, and an a posteriori probability map is made iteratively. The final segmentation is based on the a posteriori probability maps, and information from all slices are taken into account. The Department of Cardiology at Stavanger University Hospital provided LGE-CMR images of 54 patients, all with previous myocardial infarction. CMR was performed using 1.5 T Philips Intera R 8.3, pixel size of 0.82×0.82mm^2, covering the whole ventricle with short-axis slices of 10 mm thickness, without inter-slice gaps. An example of all the 8 slices from one patient is seen in Figure 1, and the epicardium is the outer border of the dark ring (partly bright because of scar) approximately in the middle of each slice.

2. Proposed method

Let $f^i(x), \quad i = 1 \ldots N_{slice}$ represent the left ventricle short axis LGE-CMR images of a patient. $x = [x_{row} \;\; x_{column}]^T$ is the pixel position, and i represents

Algorithm 1: Iterative probability map algorithm

Data: CMR images $f^i(x) \in \mathcal{R}^{M\times N}$, Prior prob. map $p_0^i(x) \in \mathcal{R}^{N\times M}$ $i = 1, \ldots, N_{slice}$,
Result: Posteriori prob. map, $p_{post}^i(x) \in \mathcal{R}^{N\times M}, i = 1, \ldots, N_{slice}$

initialization: k_{final};
for $i \leftarrow 1$ **to** N_{slice} **do**
  $f_{prep}^i(x) \leftarrow \beta_{B_{mc}}(f^i)$ %morph noise removal;
  $f_{inv}^i(x) =$scale$(ones(N, M) - f_{prep}^i(x))$;
end for
for $k \leftarrow 0$ **to** $k_{final} - 1$ **do**
  $f_{temp}(x) = p_k(x) \circ f_{inv}(x)$;
  $f_{temp}(x) \leftarrow LPfiltZ(f_{temp}(x))$ %filter slices;
  $p_{k+1}(x) \leftarrow$ scale$(f_{temp}(x))$;
end for
$p2(x) = p_0(x) \circ (f_{inv}(x))^{\circ(k_{final})}$;
$p_{post}(x) =$ scale$(p_{k_{final}}(x) + p2(x))$;
$return(p_{post})$;

the slice number. We define the morphological operations [5] of dilation and erosion as $[\delta_B f](x)$ and $[\epsilon_B f](x)$ respectively, where $B(x)$ is a structuring element, and opening and closing as $\gamma_B(f) = \delta_B(\epsilon_B(f))$ and $\phi_B(f) = \epsilon_B(\delta_B(f))$ respectively. Morphological center, $(\beta(f))$, is a morphological filter used in our preprocessing algorithms defined as:

$$\beta_{B_{mc}}(f)(x) = \min(\max(f(x), f_1(x)), f_2(x)) \qquad (1)$$

where $f_1(x) = \gamma_{B_{mc}}(\phi_{B_{mc}}(\gamma_{B_{mc}}(f)))$ and $f_2(x) = \phi_{B_{mc}}(\gamma_{B_{mc}}(\phi_{B_{mc}}(f)))$. In geodesic transformations two images are required, the reference $f(x)$ and the marker $g(x)$. The morphological reconstruction, $\gamma^{rec}(g, f)$, or reconstruction by dilation is the successive geodesic dilation of the marker regarding the reference up to idempotence [5]. Using the morphological reconstruction, we can define the close-hole operator which fills all holes in a gray-scale image $f(x)$ that do not touch the image border, $f_{border}(x)$, defined as: $f_{border}(x) = f(x)$, for $x \in \{x_{border}\}$ and 0 everywhere else.

$$\phi^{ch}(f) = [\gamma^{rec}(f^c(x), f_{border}(x))], \qquad (2)$$

where $f^c(x)$ denotes the inverse of the image $f(x)$.

2.1. A priori probability map

Some general knowledge of the nature of the myocardium needs to be exploited. We are only considering left ventricle short axis slices, and in these images the myocardial muscle has the approximated shape of a ring. Typical sizes of the endocardium and epicardium is also known. We propose to make a crude a priori model of the heart using a Gaussian prior in the radial direction from the heart center for every possible angle $\theta \in [0 - 2\pi]$:

$$p_\theta(r) = \frac{1}{\sqrt{2\pi\sigma^2}} e^{\frac{(r-\mu_i)^2}{2\sigma^2}} \qquad (3)$$

where μ_i is the a priori radius at slice number i according to knowledge of a typical heart size, and σ is the variance, and the same for all slices. In the experiments $\sigma = 15$ and $\mu = [16\ 24\ 29\ 32\ 35\ 35 \ldots 35\ 34]^T$ pixels. Converting from polar to cartesian for all radii (within interest) and all angles, and thereafter quantize to form a digital image and scaled to make all pixel values $\in [0, 1]$, a 2D *probability for being myocardium map* is made $p_0^i(x)$. The approximated center of the heart is an important input to make the a priori probability map. We define $HC_j^i = [HC_{row}\ HC_{column}]^T$ as the heart center for patient j in slice i. In our previous work [6] two alternative methods to find the heart center is proposed, one based on morphological preprocessing followed by the Circular Hough Transform (CHT), and another method based on the morphological method of grey level distance, both performing very good.

2.2. A posteriori probability map

Using the a priori probability map as input, we propose an iterative approach to refine the map and make an a posteriori probability map for the myocardium. At each iteration the probability map is combined with the inverse of the original (preprocessed) slices. The inverse is used since the myocardium has very low values in the images, and we want to express the probability of being myocardium. A filtering over the neighboring slices is performed an the output is scaled to a new probability map. The final probability map is a weighted sum between one version filtering over the neighboring slices in every iteration, and another with no filtering. Without filtering over the slices, the a posteriori map can be found directly as $p2(x) = p_0(x) \circ (f_{inv}(x))^{\circ(k_{final})}$, where $A \circ B$ denotes the Hademard product, and $A^{\circ(k)}$ denotes the Hadamard product of A with itself k times. A pseudo code of the algorithm is depicted in Algorithm 1, where scale(A) set all values in $A \in [0, 1]$. An example of the a priori map and a posteriori map of a patient can be seen in figure 2.

2.3. Segmentation of epicardium

The final segmentation step is challenging. The patients (all) have myocardial scars which appears as bright areas whereas the healthy parts of the myocardial muscle appears dark. Therefore scarred areas might be very dark in the a posteriori probability images and the intensity levels are very uneven at different angles. Thus a global thresholding technique will not work. We need to evaluate the

different probability levels radially at each possible angle instead. To simplify and spatially smooth the probability map, it is quantized using an Otsu's thresholding based method (slice by slice) for nonuniform quantization with 5 bins, giving $f_q^i(x)$. Using the position HC_j^i as origin, the values from $f_q^i(x)$ are interpreted in polar coordinates giving $f_{q_{pol}}^i(\theta, r)$. The partial derivative of $f_{q_{pol}}^i(\theta, r)$ with respect to r is found for all θ, $D_r(\theta, r)$, and the first negative value of the derivative (smallest radius) is marked as a candidate epicardium border point, $R_{epi}^i(\theta)$, for each θ. For some angles the algorithm will fail to find such a point, and an alternative is found interpolated from the other slices and from the other angles. Finally the convex hull of the candidate borders is found giving the epicardium mask, $Mask_{epicard}(x)$.

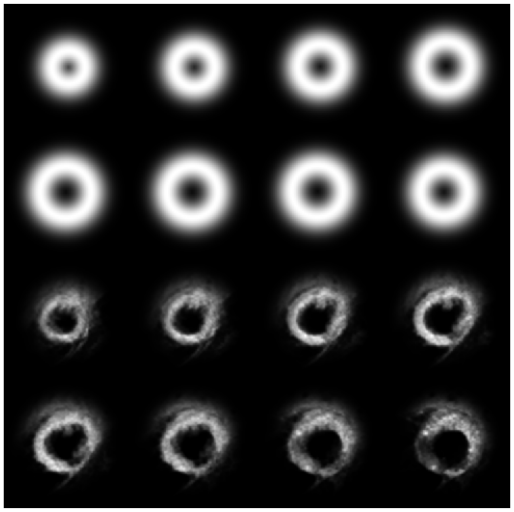

Figure 2. A priori and a posteriori probability map of all slices of a patient.

Algorithm 2: Final segmentation of epicardium

Data: CMR images, $f^i(x) \in \mathcal{R}^{N \times M}$, a post prob. map, $p_{post}^i(x) \in \mathcal{R}^{N \times M}$, $i = 1, \ldots N_{slice}$, heart center coordinates HC_i;
Result: $Mask_{epicard}^i(x)$

initialization: $R_{epi}^i(\theta) = 0,\ \theta \in [0, 2\pi]$;
$f_{ch}(x) = \phi^{ch}(p_{post}(x))$;
for $i = 1$ **to** N_{slice} **do**
  $f_q^i(x) = Quant_{nonuni}^i(f_{ch}^i(x), L)$ % Nonuniform quantization in L bins ;
  for $\theta = 0$ **to** 2π **do**
    $f_{q_{pol}}^i(\theta, r) =$ car2polar$(f_q^i(x), \theta, HC_i)$;
    $D_r(\theta, r) = \frac{\delta f_{q_{polar}}^i(\theta, r)}{\delta r}$;
    $R_{epi}(\theta) = argmin_r(D_r < 0)$;
  end for
  $R_{epi}^i(\theta) \leftarrow smooth(R_{epi}^i(\theta))$;
end for
for $i = 1$ **to** N_{slice} **do**
  for $\theta = 0$ **to** 2π **do**
    if $R_{epi}^i(\theta) = 0$ **then**
      $R_{epi}^i(\theta) \leftarrow mean(R_{epi}^j(\theta) \neq 0)$
    end if
    if $R_{epi}^i(\theta) = 0$ **then**
      $R_{epi}^i(\theta) \leftarrow min_{|\Delta_\theta|}(R_{epi}^i(\theta - \Delta_\theta) \neq 0)$
    end if
    $x_\theta^i = poly2cart(R_{epi}^i(\theta))$;
    $f_p^i(x_\theta^i) = 1$;
  end for
  $Mask_{epicard}^i(x) = ConvexHull(f_p^i(x))$;
end for
$return(Mask_{epicard}(x))$;

2.4. Postprocessing

Postprocessing is done excluding parts of the $Mask_{epicard}^i(x)$ *not present* in any of the other slices, $Mask_{epicar}^j(x)$, for all $j \neq i$, and including parts in $Mask_{epicard}^i(x)$ *present* in all other slices $Mask_{epicar}^j(x)$, for all $j \neq i$. An additional postprocessing is low-pass filtering of the Fourier Descriptor (FD) of the boundary, giving a new mask $MaskFD_{epicard}^i(x)$.

3. Experiments and results

The method is tested on all 54 patients, 503 images, and evaluated compared to consensus manual segmentation of two experienced cardiologists (LW,SØ). The input is the full images, as seen in Figure 1. Firstly the approximated heart centers, HC_j are found using the Circular Hough Transform (CHT) method presented in [6]. The images are automatically cropped to a region of interest based on the HC_j. Subsequently the a posteriori probability maps are found from the iterative probability map algorithm, 1, followed by the final segmentation algorithm 2. The number of iterations $k_{final} = 8$ was chosen empirically. The low-pass filter, performed pixel by pixel over the slices, $LPfiltZ(f_{temp}(x))$, is a simple anti causal FIR filter: $H(z) = 0.15z^{-1} + 0.7 + 0.15z^1$. The results are evaluated by the Dice index and the Jaccard index, as well as visually. The first and last slice of each patient in the data material are of poor quality. They are used in the algorithm, filtering over slices, but they are excluded from the evaluation and in the figures, leaving 395 images for

evaluation.

The mean and variance of the Dice and Jaccard indices over the entire set can be seen in Table 1. Results are seen without (first column) and with (second and third column) the FD post processing. Third column shows the results when the true heart center is given as input, indicating how well the proposed iterative probability map and final segmentation step performs in case of a perfect heart center input algorithm. Figure 3 shows the result of all slices of an example patient. Figure 4 illustrates a problem that sometimes occurs in slices with large scars. Figure 5 illustrates a problem that sometimes occurs if the a priori model fits badly. This can be because the automatically found heart center is not in the center even if it is always inside the endocardium, or if the size of the heart is very different from the a priori model heart.

Table 1. Jaccard and Dice index av. over 395 images

	Epicard	Epicard FD	True HC (FD)
Dice mean	0.86	0.86	0.90
Dice var	0.0029	0.0027	0.0012
Jaccard mean	0.76	0.76	0.81
Jaccard var	0.0062	0.0060	0.0030

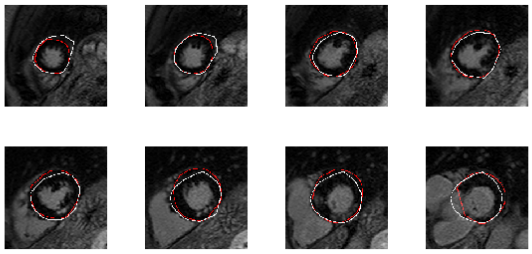

Figure 3. Example result of a patient in white, doctors manual marking in red. Dice=0.93, Jaccard=0.86.

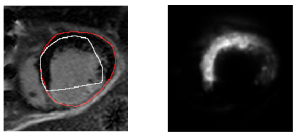

Figure 4. Example where the large scar make the result poor. Markings on original image at left, and a posteriori probability map at right.

4. Conclusion and future work

Automatic segmentation of LGE CMR images without additional information of anatomical landmarks or cine CMR, remains a difficult task. However the presented results are encouraging with mean dice index at 0.86 over a set of 54 patients and 395 images. There are some issues related to a mismatch with the a priori model that we want to improve. We are currently working on segmentation of the endocardium as well.

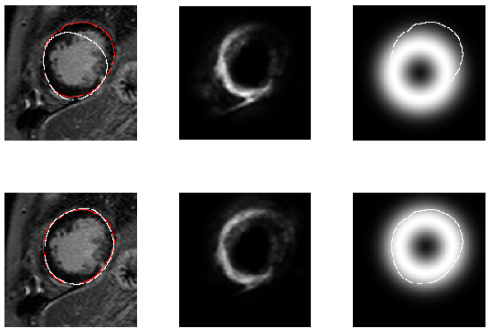

Figure 5. Example where the a priori model fits badly because of skewed HC. Upper line all automatic, lower line true HC used as input. from left: markings, a posteriori prob. map, a priori model with true marking superimposed.

References

[1] de Bruijne M, Nielsen M. Shape particle filtering for image segmentation. In Proc. of MICCAI, volume 3216. 2004; 168–175.

[2] Spreeuwers L, Breeuwer M. Detection of left ventricular and epi- and endocardial borders using coupled active contours. In Proc. Comput. Assisted Radiol. Surg. 2003; 11471152.

[3] ODonnell T, Xu N, Setser R, White R. Semi-automatic segmentation of nonviable cardiac tissue using cine and delayed enhancement magnetic resonance images. In Proceedings of SPIE 2003, volume 5031. 2003; 242.

[4] Wei D, Sun Y, Chai P, Low A, Ong S. Myocardial segmentation of late gadolinium enhanced mr images by propagation of contours from cine mr images. Med Image Comput Comput Assist Interv 2011;14:428–35.

[5] Serra J. Image Analysis and Mathematical Morphology, volume 1. London: Ac. Press,, 1989.

[6] K.Engan, Naranjo V, Eftestøl T, Woie L, Schuchter A, Ørn S. Automatic detection of heart center in late gadolinium enhanced MRI. In Proceedings of MEDICON 2013. Sevilla, Spain, September 2013; .